Exploring Synchronization in Complex Oscillator Networks

Florian Dörfler Francesco Bullo

***Abstract*— The emergence of synchronization in a network of coupled oscillators is a pervasive topic in various scientific disciplines ranging from biology, physics, and chemistry to social networks and engineering applications. A coupled oscillator network is characterized by a population of heterogeneous oscillators and a graph describing the interaction among the oscillators. These two ingredients give rise to a rich dynamic behavior that keeps on fascinating the scientific community. In this article, we present a tutorial introduction to coupled oscillator networks, we review the vast literature on theory and applications, and we present a collection of different synchronization notions, conditions, and analysis approaches. We focus on the canonical phase oscillator models occurring in countless real-world synchronization phenomena, and present their rich phenomenology. We review a set of applications relevant to control scientists. We explore different approaches to phase and frequency synchronization, and we present a collection of synchronization conditions and performance estimates. For all results we present self-contained proofs that illustrate a sample of different analysis methods in a tutorial style.**

I. Introduction

The scientific interest in synchronization of coupled oscillators can be traced back to the work by Christiaan Huygens on "an odd kind sympathy" between coupled pendulum clocks [1], and it still fascinates the scientific community nowadays [2], [3]. Within the rich modeling phenomenology on synchronization among coupled oscillators, we focus on the canonical model of a continuous-time limit-cycle oscillator network with continuous and bidirectional coupling.

A network of coupled phase oscillators: A mechanical analog of a coupled oscillator network is the spring network shown in Figure 1 and consists of a group of kinematic particles constrained to rotate around a circle and assumed to move without colliding. Each particle is characterized by a phase angle $\theta_i \in \mathbb{S}^1$ and has a preferred natural rotation frequency $\omega_i \in \mathbb{R}$. Pairs of interacting particles i and j are coupled through an elastic spring with stiffness $a_{ij} > 0$. We refer to the Appendix A for a first principle modeling of the spring-interconnected particles depicted in Figure 1.

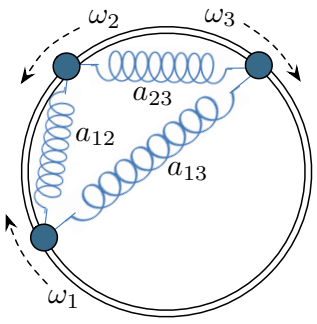

Fig. 1. Mechanical analog of a coupled oscillator network

This material is based in part upon work supported by NSF grants IIS-0904501 and CPS-1135819.

Florian Dörfler and Francesco Bullo are with the Center for Control, Dynamical Systems and Computation, University of California at Santa Barbara. Email: {dorfler,bullo}@engineering.ucsb.edu

Formally, each isolated particle is an oscillator with first-order dynamics $\dot{\theta}_i = \omega_i$. The interaction among n such oscillators is modeled by a connected graph $G(\mathcal{V}, \mathcal{E}, A)$ with nodes $\mathcal{V} = \{1, \dots, n\}$, edges $\mathcal{E} \subset \mathcal{V} \times \mathcal{V}$, and positive weights $a_{ij} > 0$ for each undirected edge $\{i, j\} \in \mathcal{E}$. Under these assumptions, the overall dynamics of the coupled oscillator network are

$$\dot{\theta}_i = \omega_i - \sum_{j=1}^{n} a_{ij} \sin(\theta_i - \theta_j), \qquad i \in \{1, \dots, n\}. \quad (1)$$

The rich dynamic behavior of the coupled oscillator model (1) arises from a competition between each oscillator's tendency to align with its natural frequency ω_i and the synchronization-enforcing coupling $a_{ij} \sin(\theta_i - \theta_j)$ with its neighbors. Intuitively, a weakly coupled and strongly heterogeneous network does not display any coherent behavior, whereas a strongly coupled and sufficiently homogeneous network is amenable to synchronization, where all frequencies $\dot{\theta}_i(t)$ or even all phases $\theta_i(t)$ become aligned.

History, applications and related literature: The coupled oscillator model (1) has first been proposed by Arthur Winfree [4]. In the case of a complete interaction graph, the coupled oscillator dynamics (1) are nowadays known as the *Kuramoto model* of coupled oscillators due to Yoshiki Kuramoto [5], [6]. Stephen Strogatz provides an excellent historical account in [7]. We also recommend the survey [8].

Despite its apparent simplicity, the coupled oscillator model (1) gives rise to rich dynamic behavior. This model is encountered in various scientific disciplines ranging from natural sciences over engineering applications to social networks. The model and its variations appear in the study if biological synchronization phenomena such as pacemaker cells in the heart [9], circadian rhythms [10], neuroscience [11]–[13], metabolic synchrony in yeast cell populations [14], flashing fireflies [15], chirping crickets [16], biological locomotion [17], animal flocking behavior [18], fish schools [19], and rhythmic applause [20], among others. The coupled oscillator model (1) also appears in physics and chemistry in modeling and analysis of spin glass models [21], [22], flavor evolutions of neutrinos [23], coupled Josephson junctions [24], and in the analysis of chemical oscillations [25].

Some technological applications of the coupled oscillator model (1) include deep brain stimulation [26], [27], vehicle coordination [19], [28]–[31], carrier synchronization without

phase-locked loops [32], semiconductor lasers [33], [34], microwave oscillators [35], clock synchronization in decentralized computing networks [36]–[41], decentralized maximum likelihood estimation [42], and droop-controlled inverters in microgrids [43]. Finally, the coupled oscillator model (1) also serves as the prototypical example for synchronization in complex networks [44]–[47] and its linearization is the well-known consensus protocol studied in networked control, see the surveys and monographs [48]–[50]. Various control scientists explored the coupled oscillator model (1) as a nonlinear generalization of the consensus protocol [51]–[57].

Second-order variations of the coupled oscillator model (1) appear in synchronization phenomena, in population of flashing fireflies [58], in particle models mimicking animal flocking behavior [59], [60], in structure-preserving power system models, [61], [62] in network-reduced power system models [63], [64], in coupled metronomes [65], in pedestrian crowd synchrony on London's Millennium bridge [66], and in Huygen's pendulum coupled clocks [67]. Coupled oscillator networks with second-order dynamics have been theoretically analyzed in [8], [68]–[74], among others.

Coupled oscillator models of the form (1) are also studied from a purely theoretic perspective in the physics, dynamical systems, and control communities. At the heart of the coupled oscillator dynamics is the transition from incoherence to synchrony. Here, different notions and degrees of synchronization can be distinguished [74]–[76], and the (apparently) incoherent state features rich and largely unexplored dynamics as well [47], [77]–[79]. In this article we will be particularly interested in phase and frequency synchronization when all phases $\theta_i(t)$ become aligned, respectively all frequencies $\dot{\theta}_i(t)$ become aligned. We refer to [7], [8], [19], [28], [31], [52], [53], [56], [64], [74]–[76], [80]–[95], [95]–[114] for an incomplete overview concerning numerous recent research activities. We will review some of literature throughout the paper and refer to the surveys [7], [8], [44]–[46], [74] for further applications and numerous additional theoretic results concerning the coupled oscillator model (1).

Contributions and contents: In this paper, we introduce the reader to synchronization in networks of coupled oscillators. We present a sample of important analysis concepts in a tutorial style and from a control-theoretic perspective.

In Section II, we will review a set of selected technological applications which are directly tied to the coupled oscillator model (1) and also relevant to control systems. We will cover vehicle coordination, electric power networks, and clock synchronization in depth, and also justify the importance of the coupled oscillator model (1) as a canonical model. Prompted by these applications, we review the existing results concerning phase synchronization, phase balancing, and frequency synchronization, and we also present some novel results on synchronization in sparsely-coupled networks.

In particular, Section III introduces the reader to different synchronization notions, performance metrics, and synchronization conditions. We illustrate these results with a simple yet rich example that nicely explains the basic phenomenology in coupled oscillator networks.

Section IV presents a collection of important results regarding phase synchronization, phase balancing, and frequency synchronization. By now the analysis methods for synchronization have reached a mature level, and we present simple and self-contained proofs using a sample of different analysis methods. In particular, we present one result on phase synchronization and one result on phase balancing including estimates on the exponential synchronization rate and the region of attraction (see Theorem 4.3 and Theorem 4.4). We also present some implicit and explicit, and necessary and sufficient conditions for frequency synchronization in the classic homogeneous case of a complete and uniformly-weighted coupling graphs (see Theorem 4.5). Concerning frequency synchronization in sparse graphs, we present two partially new synchronization conditions depending on the algebraic connectivity (see Theorem 4.6 and Theorem 4.7).

In our technical presentation, we try to strike a balance between mathematical precision and removing unnecessary technicalities. For this reason some proofs are reported in the appendix and others are only sketched here with references to the detailed proofs elsewhere. Hence, the main technical ideas are conveyed while the tutorial value is maintained.

Finally, Section V concludes the paper. We summarize the limitations of existing analysis methods and suggest some important directions for future research.

Preliminaries and notation: The remainder of this section introduces some notation and recalls some preliminaries.

Vectors and functions: Let $\mathbf{1}_n$ and $\mathbf{0}_n$ be the n-dimensional vector of unit and zero entries, and let $\mathbf{1}_n^\perp$ be the orthogonal complement of $\mathbf{1}_n$ in $\mathbb{R}^n$, that is, $\mathbf{1}_n^\perp \triangleq \{x \in \mathbb{R}^n : x \perp \mathbf{1}_n\}$. Given an n-tuple $(x_1, \dots, x_n)$, let $x \in \mathbb{R}^n$ be the associated vector with maximum and minimum elements $x_{\max}$ and $x_{\min}$. For an ordered index set $\mathcal{I}$ of cardinality $|\mathcal{I}|$ and an one-dimensional array $\{x_i\}_{i\in\mathcal{I}}$, let $\operatorname{diag}(\{c_i\}_{i\in\mathcal{I}}) \in \mathbb{R}^{|\mathcal{I}|\times|\mathcal{I}|}$ be the associated diagonal matrix. Finally, define the continuous function $\operatorname{sinc} : \mathbb{R} \to \mathbb{R}$ by $\operatorname{sinc}(x) = \sin(x)/x$ for $x \neq 0$.

Geometry on the n-torus: The set $\mathbb{S}^1$ denotes the *unit circle*, an *angle* is a point $\theta \in \mathbb{S}^1$, and an *arc* is a connected subset of $\mathbb{S}^1$. The *geodesic distance* between two angles θ_1, $\theta_2 \in \mathbb{S}^1$ is the minimum of the counter-clockwise and the clockwise arc lengths connecting θ_1 and θ_2. With slight abuse of notation, let $|\theta_1 - \theta_2|$ denote the *geodesic distance* between two angles $\theta_1, \theta_2 \in \mathbb{S}^1$. The *$n$-torus* is the product set $\mathbb{T}^n = \mathbb{S}^1 \times \cdots \times \mathbb{S}^1$ is the direct sum of n unit circles. For $\gamma \in [0, 2\pi[$, let $\overline{\operatorname{Arc}}_n(\gamma) \subset \mathbb{T}^n$ be the closed set of angle arrays $\theta = (\theta_1, \dots, \theta_n)$ with the property that there exists an arc of length γ containing all $\theta_1, \dots, \theta_n$. Thus, an angle array $\theta \in \overline{\operatorname{Arc}}_n(\gamma)$ satisfies $\max_{i,j\in\{1,\dots,n\}} |\theta_i - \theta_j| \leq \gamma$. Finally, let $\operatorname{Arc}_n(\gamma)$ be the interior of the set $\overline{\operatorname{Arc}}_n(\gamma)$.

Algebraic graph theory: Let $G(\mathcal{V}, \mathcal{E}, A)$ be an undirected, connected, and weighted graph without self-loops. Let $A \in \mathbb{R}^{n\times n}$ be its symmetric nonnegative *adjacency matrix* with zero diagonal, $a_{ii} = 0$. For each node $i \in \{1, \dots, n\}$, define the nodal degree by $\deg_i = \sum_{j=1}^n a_{ij}$. Let $L \in \mathbb{R}^{n\times n}$ be the *Laplacian matrix* defined by $L = \operatorname{diag}(\{\deg_i\}_{i=1}^n) - A$. If a number $\ell \in \{1, \dots, |\mathcal{E}|\}$ and an arbitrary direction is assigned to each edge $\{i, j\} \in \mathcal{E}$, the (oriented) *incidence*

matrix $B \in \mathbb{R}^{n\times|\mathcal{E}|}$ is defined component-wise by $B_{k\ell} = 1$ if node k is the sink node of edge ℓ and by $B_{k\ell} = -1$ if node k is the source node of edge ℓ; all other elements are zero. For $x \in \mathbb{R}^n$, the vector $B^T x$ has components $x_i - x_j$ corresponding to the oriented edge from j to i, that is, B^T maps node variables x_i, x_j to incremental edge variables $x_i - x_j$. If $\mathrm{diag}(\{a_{ij}\}_{\{i,j\}\in\mathcal{E}})$ is the diagonal matrix of edge weights, then $L = B\,\mathrm{diag}(\{a_{ij}\}_{\{i,j\}\in\mathcal{E}})B^T$. If the graph is connected, then $\mathrm{Ker}\,(B^T) = \mathrm{Ker}\,(L) = \mathrm{span}(\mathbf{1}_n)$, all $n-1$ non-zero eigenvalues of L are strictly positive, and the second-smallest eigenvalue $\lambda_2(L)$ is called the *algebraic connectivity* and is a spectral connectivity measure.

II. Applications of Kuramoto Oscillators Relevant to Control Systems

The mechanical analog in Figure 1 provides an intuitive illustration of the coupled oscillator dynamics (1), and we reviewed a wide range of examples from physics, life sciences, and technology in Section I. Here, we detail a set of selected technological applications which are relevant to control systems scientists.

A. Flocking, Schooling, and Planar Vehicle Coordination

An emerging research field in control is the coordination of autonomous vehicles based on locally available information and inspired by biological flocking phenomena. Consider a set of n particles in the plane $\mathbb{R}^2$, which we identify with the complex plane $\mathbb{C}$. Each particle $i \in \mathcal{V} = \{1,\dots,n\}$ is characterized by its position $r_i \in \mathbb{C}$, its heading angle $\theta_i \in \mathbb{S}^1$, and a steering control law $u_i(r,\theta)$ depending on the position and heading of itself and other vehicles. For simplicity, we assume that all particles have constant and unit speed. The particle kinematics are then given by [115]

$$\left.\begin{aligned} \dot r_i &= e^{\mathrm{i}\theta_i}\,,\\ \dot\theta_i &= u_i(r,\theta)\,, \end{aligned}\right\} \quad i\in\{1,\dots,n\}\,, \tag{2}$$

where $\mathrm{i} = \sqrt{-1}$ is the imaginary unit. If the control u_i is identically zero, then particle i travels in a straight line with orientation $\theta_i(0)$, and if $u_i = \omega_i \in \mathbb{R}$ is a nonzero constant, then the particle traverses a circle with radius $1/|\omega_i|$.

The interaction among the particles is modeled by a possibly time-varying interaction graph $G(\mathcal{V},\mathcal{E}(t),A(t))$ determined by communication and sensing patterns. Some interesting motion patterns emerge if the controllers use only relative phase information between neighboring particles, that is, $u_i = \omega_0(t) + f_i(\theta_i - \theta_j)$ for $\{i,j\} \in \mathcal{E}(t)$ and $\omega_0 : \mathbb{R}_{\geq 0} \to \mathbb{R}$. For example, the control $u_i = \omega_0(t) - K\cdot\sum_{j=1}^n a_{ij}(t)\sin(\theta_i-\theta_j)$ with gain $K\in\mathbb{R}$ results in

$$\dot\theta_i = \omega_0(t) - K\cdot\sum\nolimits_{j=1}^n a_{ij}(t)\sin(\theta_i-\theta_j)\,,\quad i\in\mathcal{V}\,. \tag{3}$$

The controlled phase dynamics (3) correspond to the coupled oscillator model (1) with a time-varying interaction graph with weights $K\cdot a_{ij}(t)$ and identically time-varying natural frequencies $\omega_i = \omega_0(t)$ for all $i\in\{1,\dots,n\}$. The controlled phase dynamics (3) give rise to very interesting coordination patterns that mimic animal flocking behavior [18] and fish schools [19]. Inspired by these biological phenomena, the controlled phase dynamics (3) and its variations have also been studied in the context of tracking and formation controllers in swarms of autonomous vehicles [19], [28]–[31]. A few trajectories are illustrated in Figure 2, and we refer to [19], [28]–[31] for other control laws and motion patterns.

In the following sections, we will present various tools to analyze the motion patterns in Figure 2, which we will refer to as *phase synchronization* and *phase balancing*.

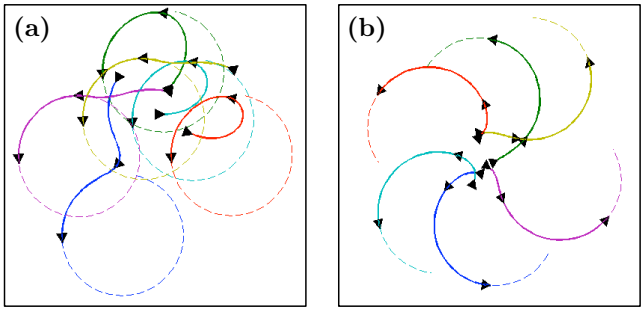

Fig. 2. Illustration of the controlled dynamics (2)-(3) with $n=6$ particles, a complete interaction graph, and identical and constant natural frequencies $\omega_0(t) = 1$, where $K = 1$ in panel (a) and $K = -1$ in panel (b). The arrows depict the orientation, the dashed curves show the long-term position dynamics, and the solid curves show the initial transient position dynamics. It can be seen that even for this simple choice of controller, the resulting motion results in "synchronized" or "balanced" heading angles for $K = \pm 1$.

B. Power Grids with Synchronous Generators and Inverters

Here, we present the *structure-preserving power network model* introduced in [61] and refer to [62, Chapter 7] for detailed derivation from a higher order first principle model. Additionally, we equip the power network model with a set of inverters and refer to [43] for a detailed modeling.

Consider an alternating current (AC) power network modeled as an undirected, connected, and weighted graph with node set $\mathcal{V} = \{1,\dots,n\}$, transmission lines $\mathcal{E}\subset\mathcal{V}\times\mathcal{V}$, and admittance matrix $Y = Y^T \in \mathbb{C}^{n\times n}$. For each node, consider the voltage phasor $V_i = |V_i|e^{\mathrm{i}\theta_i}$ corresponding to the phase $\theta_i \in \mathbb{S}^1$ and magnitude $|V_i| \geq 0$ of the sinusoidal solution to the circuit equations. If the network is lossless, then the active power flow from node i to j is $a_{ij}\sin(\theta_i-\theta_j)$, where we used the shorthand $a_{ij} = |V_i|\cdot|V_j|\cdot\Im(Y_{ij})$.

In the following, we assume that the node set is partitioned as $\mathcal{V} = \mathcal{V}_1\cup\mathcal{V}_2\cup\mathcal{V}_3$, where $\mathcal{V}_1$ are load buses, $\mathcal{V}_2$ are conventional synchronous generators, and $\mathcal{V}_3$ are grid-connected direct current (DC) power sources, such as solar farms. The active power drawn by a load $i\in\mathcal{V}_1$ consists of a constant term $P_{\mathrm{l},i} > 0$ and a frequency-dependent term $D_i\dot\theta_i$ with $D_i > 0$. The resulting power balance equation is

$$D_i\dot\theta_i + P_{\mathrm{l},i} = -\sum\nolimits_{j=1}^n a_{ij}\sin(\theta_i-\theta_j)\,,\quad i\in\mathcal{V}_1\,. \tag{4}$$

If the generator reactances are absorbed into the admittance matrix, then the swing dynamics of generator $i\in\mathcal{V}_2$ are

$$M_i\ddot\theta_i + D_i\dot\theta_i = P_{\mathrm{m},i} - \sum\nolimits_{j=1}^n a_{ij}\sin(\theta_i-\theta_j)\,,\quad i\in\mathcal{V}_2, \tag{5}$$